

Killing three birds with one stone—simultaneous operando EPR/UV-vis/Raman spectroscopy for monitoring catalytic reactions

Angelika Brückner

Received (in Cambridge, UK) 15th December 2004, Accepted 25th January 2005

First published as an Advance Article on the web 4th February 2005

DOI: 10.1039/b418790c

For the first time, three operando methods, namely EPR, UV-vis and laser-Raman spectroscopy have been applied in parallel on the same V/TiO₂ catalyst and under identical reaction conditions during oxidative dehydrogenation of propane to elucidate structure–reactivity relationships *in status operandi*.

A recent trend of growing importance in catalysis research comprises the monitoring of catalysts under reaction conditions, including analysis of product composition, *i.e.*, *in status operandi*, by more than one operando technique at the same time and in the same reactor. The crucial advantage of such multiple couplings is the fact that results are obtained from the very same catalyst sample for which identical reaction conditions are guaranteed. Thus, the spectroscopic responses from different methods can be directly interrelated which may provide more comprehensive and more relevant results. This is not possible without doubt when, as usual so far, the experiments are performed with different samples (though from the same batch) in different reaction cells, since identical reaction conditions, in particular, with respect to reactant flow and temperature distribution within the samples are not ensured. This communication illustrates the special benefits obtained by using operando EPR/UV-vis-DRS/laser-Raman spectroscopy—the first threefold coupling of operando techniques—for analysis of structure–function relationships during the oxidative dehydrogenation of propane (ODP).

For performing such triple operando experiments, the previously established set-up for simultaneous operando EPR/UV-vis spectroscopy consisting of a fibre optical sensor implemented into an EPR fixed-bed flow reactor¹ has been extended by focusing the beam of a 785 nm diode laser of a Kaiser Optical Systems RXN spectrometer through a front hole in the EPR cavity onto the catalyst bed within the reactor. Different from the previous set-up,¹ heat was transferred to the reactor by a stream of N₂ which was pre-heated by passing over an electrical heater. Heater power and N₂ flow rate were controlled by a Bruker variable temperature control unit. Details of spectra acquisition have been described elsewhere,¹ however, UV-vis spectra in the present work were recorded by an AVASPEC fibre optical spectrometer (Avantes) and a 200 × 1.5 mm quartz sensor (Optran UV 1500/1800 T, CeramOptec GmbH). Raman spectra were recorded with a laser power of 25 mW and an acquisition time of 3 s. Five scans were accumulated for each spectrum. Computer simulation of EPR spectra was performed with the program SIM14S of Lozos *et al.*² using the spin Hamiltonian

$$H = \mu_B S g B_0 + S A I \quad (1)$$

in which μ_B is the Bohr magneton, S is the electron spin operator, g is the g tensor, B_0 is the magnetic field vector, A is the hyperfine tensor and I is the nuclear spin operator.

A 6 wt% V/TiO₂ catalyst was used which was prepared by thermal spreading of V₂O₅ on a commercial anatase carrier (80 m² g⁻¹, 2.2% sulfate, Millennium Chemicals). The appropriate amount of V₂O₅ was mixed with the support by intense grinding in an agate mortar followed by 2 h calcination in an air flow at 600 °C. This catalyst was chosen for two reasons: (i) it contains vanadium in different forms ranging from isolated, *via* oligomeric V surface species, to V₂O₅ microcrystals and thus allows conclusions to be derived on the reaction-dependent behavior of these different species simultaneously and (ii) V/TiO₂ showed superior activity in comparison to VO_x on other support materials.^{3,4} Therefore it was concluded that the V–O–Ti moiety might be the active species but no direct experimental insight was given.⁵ From the new operando EPR/UV-vis/Raman spectroscopy setup, direct evidence for the participation of TiO₂ is expected.

For operando experiments, 60 mg catalyst particles (250–355 μm) were pretreated for 30 min in an air flow at 450 °C and cooled to room temperature. Then, the catalyst was heated stepwise in a mixture of 8.3% C₃H₈, 8.3% O₂/N₂ (total flow of 24 ml min⁻¹) to different temperatures with 10 min isothermal hold at each temperature for recording the spectra and GC analyses. The reactant gas flow was mixed by a gas dosing system containing mass flow controllers (Bronckhorst). For online product analysis, the reactor outlet was connected to a GC 17AAF capillary gas chromatograph (Shimadzu) equipped with a FID and a 30 m × 0.32 mm Silicaplot column (Chrompack).

At ambient and higher temperatures, EPR is exclusively sensitive for tetravalent vanadium and can detect isolated V⁴⁺ sites in distorted octahedral and/or square-pyramidal coordination by characteristic hyperfine structure signals with axial g and A tensors besides clustered V⁴⁺O_x that give rise to a broad isotropic singlet. In contrast, Raman spectra reflect pentavalent V species only, whereby both isolated and polymeric VO_x surface species can be distinguished from crystalline V₂O₅ and TiO₂. UV-vis spectroscopy, in general, can visualize both fully oxidized V⁵⁺ by intense charge-transfer (CT) bands in the UV range as well as reduced V species by weak d–d transitions in the visible range. However, for the V/TiO₂ catalyst used in this work, UV-vis spectroscopy can provide information on V₂O₅ and reduced V species only, since the CT range of dispersed surface V⁵⁺O_x is superimposed by the strong absorption of TiO₂. Due to the described specific limitations of each technique, their simultaneous coupling is of unique advantage. In the following, a joint discussion of the results obtained from the three spectroscopic techniques is given, dependent on the reaction conditions.

The Raman spectrum of V/TiO₂ after oxidative pretreatment shows bands of crystalline anatase (marked by A), V₂O₅ microcrystals (marked by V) as well as of isolated and polymeric O=VO_x surface species at 1034 cm⁻¹ and 945 cm⁻¹, respectively (Fig. 1).^{6,7} A further band at 1024 cm⁻¹ also assigned to polymeric surface species^{7,8} might be hidden by the bands at 1034 and 996 cm⁻¹. In the corresponding EPR spectrum, a signal 1 with hyperfine structure (hfs) ($g_{\parallel} = 1.940$, $A_{\parallel} = 176.3$ G, derived by spectra simulation) being typical for VO²⁺ species in anatase⁹ is detected which arises from V sites persisting oxidative pretreatment (Fig. 2). The related UV-vis spectrum (Fig. 3) shows a broad band around 470 nm arising from a CT transition of V₂O₅ microcrystals.¹⁰ As explained above, CT bands of isolated and low polymerized VO_x species falling below 400 nm,¹⁰ are obscured by the strong absorption of TiO₂.

Upon switching to feed at 20 °C, Raman signals of crystalline V₂O₅ and TiO₂ remain unchanged while the band at 1034 cm⁻¹ disappears immediately rendering the band at 1024 cm⁻¹ well visible (Fig. 1). In EPR, hfs signal 1 increases in intensity and a new hfs signal 2 ($g_{\parallel} = 1.925$, $A_{\parallel} = 199.2$ G) appears from VO²⁺ species which must have been formed upon reduction of isolated VO³⁺ sites by propane (Fig. 2). In the Raman spectrum of oxidatively pretreated V/TiO₂ (Fig. 1), these initial VO³⁺ sites are reflected by the band at 1034 cm⁻¹ that disappears upon contact with propane. In the corresponding UV-vis spectrum (Fig. 3), the reduction of VO³⁺ to VO²⁺ leads to increasing absorbance in the range of d-d transitions of reduced V species above 500 nm. The direct interconversion of isolated VO³⁺ (Raman band at 1034 cm⁻¹) into VO²⁺ (EPR hfs signal 1 and 2, rising light absorption above 500 nm) which is simultaneously confirmed by

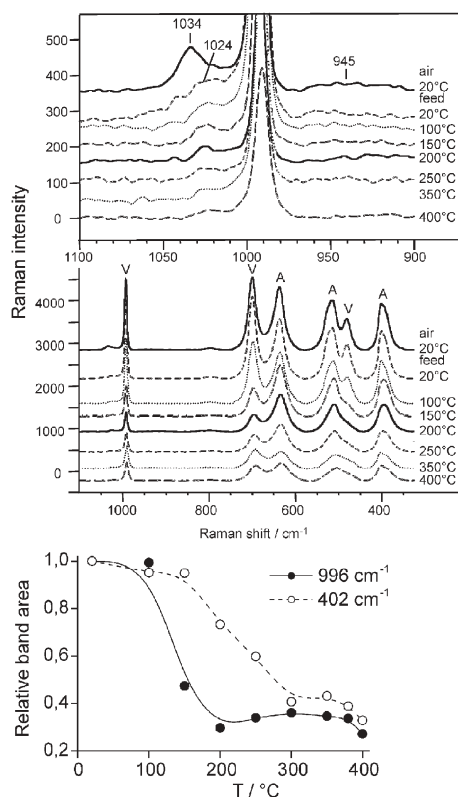


Fig. 1 Raman spectra and relative band area at 996 and 402 cm⁻¹.

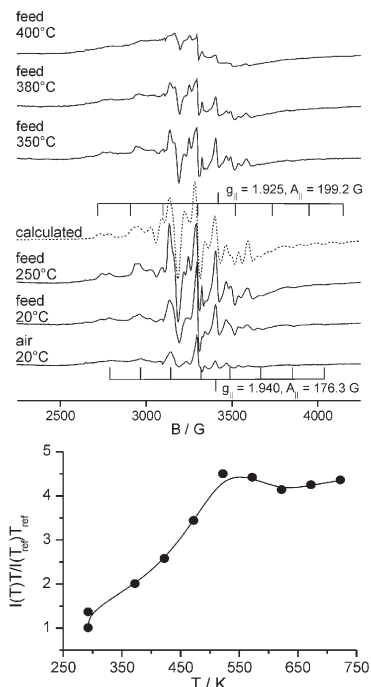


Fig. 2 EPR spectra and normalized spectral intensity ($T_{\text{ref}} = 293$ K).

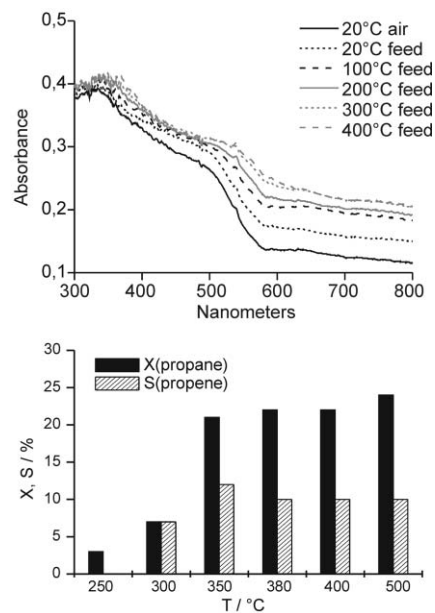


Fig. 3 UV-vis spectra and catalytic results.

all three techniques, shows clearly that isolated V⁵⁺ species on anatase are already reduced to V⁴⁺ at 20 °C. Moreover, the direct relation between the disappearance of the Raman band at 1034 cm⁻¹ and the increase of two VO²⁺ EPR lines is evidence that this Raman band cannot be exclusively due to tetrahedral O=V⁵⁺O₃ species as assumed so far^{4,7} but reflects at least two different square-pyramidal, isolated O=V⁵⁺O₄ moieties. This is unique information that could only be obtained by the triple operando approach and confirms both the previous suggestions that the V=O group gives rise to vibrations largely independent of

the rest of the molecule^{4,7} as well as the assumption that VO_x on anatase might be connected to the support by four oxygen bridges.⁶

Upon a stepwise increase of temperature, the Raman band of polymeric surface V_xO_y (1024 cm⁻¹) decreases gradually and those of V₂O₅ drop to a constant low level above 200 °C (Fig. 1). This is also evident from a plot of the relative band area derived by integration in the range between 900 and 1100 cm⁻¹ (Fig. 1). The Raman bands of anatase loose intensity, too, although more slowly and at higher temperature compared to V₂O₅. When the V-free TiO₂ support is treated under the same conditions, band intensity decreases, too, but to a markedly smaller extent. This suggests that the redox activity of the support might be enhanced by the presence of vanadia species dispersed on its surface.

In the corresponding EPR spectra (Fig. 2), a broad singlet of polymeric V⁴⁺O_x species superimposed on the VO²⁺ hfs signals grows with rising temperature which reflects the reduction of polymeric surface V⁵⁺O_x and V₂O₅ in parallel to the decreasing Raman band at 1024 cm⁻¹ and those marked with V (Fig. 1). In general, EPR signals of paramagnetic species decrease linearly with rising temperature due to the Curie–Weiss law. To eliminate this effect, the normalized intensity function $I(T)/I(T_{\text{ref}})T_{\text{ref}}$ is plotted against the absolute temperature, in which I is the double integral of the total EPR signal and T_{ref} is a reference temperature (this work: 293 K) (Fig. 2). From this plot it is evident that the amount of V⁴⁺ increases until it reaches a constant value at ≈220 °C. This is in perfect agreement with the decrease of the V⁵⁺ Raman signal area between 900 and 1100 cm⁻¹ (Fig. 1). Considering the various EPR subsignals, it appears that hfs signal 2 vanishes gradually above 250 °C. It is also not seen anymore after cooling the used catalyst to room temperature. Most probably, the respective isolated VO²⁺ sites are reduced to EPR-silent V³⁺ which might be inactive in the catalytic reaction¹¹ while the isolated VO²⁺ sites reflected by hfs signal 1 as well as the polymeric V⁴⁺ sites comprised by the broad isotropic singlet are not further reduced.

In the corresponding UV-vis spectra (Fig. 3), the increase of light absorption above 500 nm, reflecting reduced V sites, levels off between 200 and 300 °C. This agrees pretty well with EPR and Raman results described above. In general, it is not straightforward to discriminate between the effect of reduced V species and coke deposits since the latter give rise to light absorption in the same wavelength range.¹² However the almost perfect agreement of the absorbance behaviour above 500 nm in the UV-vis spectra (Fig. 3) with the behaviour of the normalized EPR intensity comprising exclusively tetravalent vanadium (Fig. 2) suggests that the UV-vis spectra reflect V reduction only, while coke deposition is negligible.

Propane conversion becomes measurable at 250 °C and increases to a constant level above 350 °C. At this temperature, virtually all monomeric and polymeric O=V⁵⁺O_x surface species and a considerable part of the V₂O₅ crystals are reduced, however, this does not suppress propane conversion. Moreover, propene

selectivity increases, too, with rising extent of V⁵⁺ reduction. In contrast to this, it has been claimed previously that propene selectivity is favoured by V⁵⁺ surface species and V₂O₅ microcrystals are not active in ODP.¹³

In summary, the above presented results illustrate that more authentic information and new insight into a well-known catalytic system such as V/TiO₂ during ODP can be obtained when simultaneous operando EPR/UV-vis/Raman spectroscopy is used instead of the respective separate operando techniques, whereby it must be stressed, that even separate operando EPR, UV-vis and Raman measurements have not been performed so far on the same V/TiO₂ catalyst during ODP. Thus, it could be shown that isolated VO²⁺ sites in slightly different octahedral and/or square-pyramidal coordination are reacting first followed by polymerized VO_x surface species and V₂O₅ crystals. The reactivity of those species has been controversially discussed so far, and highly dispersed VO_x surface species with more than four oxygen ligands were rarely considered to be involved in the reaction. Moreover, this work provides clear evidence that different V⁴⁺ species (isolated and polymeric VO²⁺ in direct contact with TiO₂ as well as VO²⁺ sites on the surface of vanadia microcrystals) dominate under the reaction conditions and are likely active sites. Finally, the participation of the TiO₂ support in the redox process has been directly shown. The onset of propane conversion at rather low temperature is most probably due to the promotion of the catalyst redox activity by participation of TiO₂.

The author thanks the Federal Ministry for Education and Research of Germany, the EU and the Federal State of Berlin (Dept. for Science, Research and Culture) for financial support.

Angelika Brückner

Institut für Angewandte Chemie Berlin-Adlershof, † P.O. Box 961156, D-12474 Berlin, Germany. E-mail: brueckner@aca-berlin.de; Fax: +49 (0)30 6392 4454; Tel: +49 (0)30 6392 4301

Notes and references

- 1 A. Brückner, *Chem. Commun.*, 2001, 2122.
- 2 G. P. Lozos, B. M. Hofman and C. G. Franz, *Quantum Chemistry Program Exchange*, 1973, no. 265.
- 3 M. A. Bañares, M. Martínez-Huerta, X. Gao, I. E. Wachs and J. L. G. Fierro, *Stud. Surf. Sci. Catal.*, 2000, **130**, 3125.
- 4 I. E. Wachs, J.-M. Jehng, G. Deo, B. M. Weckhuysen, V. Gulians and J. B. Benziger, *Catal. Today*, 1996, **32**, 47.
- 5 M. A. Bañares and I. E. Wachs, *J. Raman Spectrosc.*, 2002, **33**, 359.
- 6 G. T. Wendt, L.-J. Leu and A. T. Bell, *J. Catal.*, 1992, **134**, 479.
- 7 L. J. Burcham, G. Deo, X. Gao and I. E. Wachs, *Top. Catal.*, 2000, **11**, 12, 85.
- 8 G. G. Cortez and M. A. Bañares, *J. Catal.*, 2002, **209**, 197.
- 9 O. B. Lapina, A. A. Shubin, A. V. Nosov, E. Bosh, J. Spengler and H. Knözinger, *J. Phys. Chem. B*, 1999, **103**, 7599.
- 10 G. Centi, S. Perathoner, F. Trifirò, A. Aboukais, C. F. Aissi and M. Guelton, *J. Phys. Chem.*, 1992, **96**, 2617.
- 11 U. Bentrup, A. Brückner, C. Rüdinger and H.-J. Eberle, *Appl. Catal., A*, 2004, **269**, 237.
- 12 A. Brückner, *Phys. Chem. Chem. Phys.*, 2003, **5**, 4461.
- 13 X. Gao, J.-M. Jehng and I. E. Wachs, *J. Catal.*, 2002, **209**, 43.

† A member of the EU funded Coordination Action of Nanostructured Catalytic Oxide Research and Development in Europe (CONCORDE)